General Disclaimer

One or more of the Following Statements may affect this Document

- This document has been reproduced from the best copy furnished by the organizational source. It is being released in the interest of making available as much information as possible.

- This document may contain data, which exceeds the sheet parameters. It was furnished in this condition by the organizational source and is the best copy available.

- This document may contain tone-on-tone or color graphs, charts and/or pictures, which have been reproduced in black and white.

- This document is paginated as submitted by the original source.

- Portions of this document are not fully legible due to the historical nature of some of the material. However, it is the best reproduction available from the original submission.

GCA-TR-69-13-N

LABORATORY MEASUREMENTS OF PHOTODETACHMENT CROSS SECTIONS OF SELECTED NEGATIVE IONS

Principal Investigator: P. Warneck

GCA CORPORATION

Bedford, Massachusetts

FINAL REPORT

CONTRACT NO. NAS5-11157

PREPARED FOR

NATIONAL AERONAUTICS AND SPACE ADMINISTRATION

GODDARD SPACE FLIGHT CENTER

GREENBELT, MARYLAND

November 1969

GCA-TR-69-13-N

FINAL REPORT

for

LABORATORY MEASUREMENTS OF PHOTODETACHMENT CROSS SECTIONS OF SELECTED NEGATIVE IONS

(27 June 1968 - 26 June 1969)

Contract No. NAS5-11157

Goddard Space Flight Center

Contract Officer: R. G. Smith
Technical Monitor: Dr. A. C. Aiken, 615

Prepared by:

GCA CORPORATION
GCA TECHNOLOGY DIVISION
Bedford, Massachusetts

Project Manager: P. Warneck

for

GODDARD SPACE FLIGHT CENTER
Greenbelt, Maryland

TABLE OF CONTENTS

LABORATORY MEASUREMENTS OF PHOTODETACHMENT CROSS SECTIONS OF SELECTED NEGATIVE IONS

By Peter Warneck
GCA Corporation, GCA Technology Division
Bedford, Massachusetts

SUMMARY

Laboratory measurements of photodetachment cross sections of negative ions considered important in the D-region of the upper atmosphere are reported. An apparatus described previously, employing the radiation generated by a xenon-mercury arc, has been improved by the addition of a discharge ion source, and by modifications of the photodetachment chamber configuration. Photodetachment cross sections are given for the ions O^-, H^-, NO_2^-, O_2^- and OH^- at wavelengths from 6200 to 3000Å. Photodetachment cross sections for NO_2^- are reported for the first time. The observation of photodetachment of CO_3^- and NO_3^- has been attempted but no detachment was observed. Conclusions concerning D-region photodetachment processes and recommendations for further experiments are given.

I. INTRODUCTION

Negative ions are believed to play a significant role in the ion chemistry of the D-region of the upper atmosphere. Although attempts to measure negative ion concentrations by rocket probes have not yet led to meaningful observation, there have been many recent advances concerning the laboratory investigation of negative ion behavior. From the results, a qualitative picture of D-region ion chemistry has emerged (Ref. 1), which provides information on the expected relative abundance of a great number of ionic species.

In addition to ion reactions, photodetachment processes are considered to be important ion loss processes in the D-region of the upper atmosphere. Of particular interest is photodetachment in the near UV region of the solar spectrum, since polar cap absorption events (Ref. 2) and rocket probings of the electron density (Ref. 3) at twilight have indicated a detachment of electrons as the solar UV radiation becomes effective in the atmospheric region below 85 km altitude. In view of these factors it was desirable to extend previous measurements of photodetachment cross sections (mostly above 4000Å) further into the UV spectral region and to investigate photodetachment of atmospheric negative ions not previously subjected to measurement.

For this purpose an apparatus employing the radiation generated by a xenon-mercury arc source has been developed (Ref. 4). With this apparatus photodetachment experiments have now been performed. The results are contained in the present report. After a discussion of experimental details in the next section, photodetachment cross sections are reported in Section III. Results are given for the ions O^-, H^-, NO_2^-, O_2^- and OH^- at wavelengths from 6200 to 3000Å, and for O^- to 2500Å. Photodetachment cross sections for NO_2^- are reported for the first time. The observation of photodetachment of CO_3^- and NO_3^- was attempted but none was observed. Section IV gives conclusions concerning photodetachment in the D-region, and recommendations for further work.

II. EXPERIMENTAL APPARATUS

A. Introduction

The experimental apparatus and arrangement have been described in detail previously (Ref. 4). Briefly, negative ions are generated in a discharge source, extracted and accelerated to a speed of about 5×10^6 cm/sec, collimated, and mass separated in a 90 degree, stigmatically focusing magnetic analyzer. After passing the photodetachment chamber the ions are trapped in a Faraday cup and registered w.l. an electrometer. Light from a 2.5 kw mercury-xenon arc is chopped, dispersed by a f/1.5 grating scanning monochromator, and focused onto the ion beam such that its width selects an appropriate wavelength band from the available spectrum. Photoelectrons are withdrawn at right angles by a weak electric field and are detected with a venetian blind electron multiplier. The signal is processed by phase sensitive amplification and is displayed on a strip chart recorder.

In the course of experimentation, it was determined that modifications were required on two important components: the ion source and the photodetachment chamber. The changes and substitutions thus incorporated will be described below as a supplement to the detailed description of the overall apparatus given previously. Further details of the experimental procedure will be described subsequently.

B. Ion Sources

Initially, a duoplasmatron was employed for the production of negative ions. Tests of the duoplasmatron had shown that it can generate useful intensities of many but not all negative ions of interest (Ref. 4). However, the achieved intensities were not greater, and in many cases less than those reported to originate from a simple cold cathode glow discharge. In addition, the high pressures required for an adequate negative ion formation were detrimental to the filament of the duoplasmatron, so that its frequent replacement became necessary. For these reasons, a second ion source, based on a cold cathode discharge was desirable as a supplement to the duoplasmatron. This second source was used in most experiments. A detailed description of it is given below.

In the cold cathode source, negative ions are produced in a glow discharge, and are extracted through a small hole in the anode disc. Fite (Ref. 5) had found that an apertured disc placed on the cathode side of the anode increased the extracted ion current, if the disc was operated at a negative potential. More recently, this design was

extended by Whitlock and Bounden (Ref. 6) who incorporated a conical electrode in front of the anode. A negative potential on the conical electrode constricts the discharge at that point and concentrates it onto the anode extraction hole. The resulting gain in extracted ion current is considerable.

It is worth noting that the exact mechanism of ion formation in front of the anode is still incompletely understood. Both Fite and Whitlock and Bounden stress the importance of the striated structure of the positive column. It appears that negative ion formation occurs predominantly in a striation, and that the location of the last striation in front of the anode is critical for a favorable ion extraction. As the discharge parameters are altered, the striation moves away from the anode and the extracted negative ion intensity decreases, until a new striation appears. Then, the ion intensity increases again. Whitlock and Bounden found that in oxygen discharges, the production of O_2^- occurs mainly in the second striation, apparently by a reaction of O^- produced in the first striation.

The cold cathode ion source used in the present work was modeled after the configuration used by Whitlock and Bounden (Ref. 6). A cross section of it is shown in Figure 1. The base of the ion source is an aluminum disc whose center is hollowed out to make room for an aluminum anode cylinder, which is threaded so that its position can be adjusted. A second aluminum flange, insulated from the base of the ion source by a Teflon spacer, carries the discharge tube and the constrictor electrode. The discharge tube is made from quartz and is fastened with an epoxy cement. The cathode pin sits directly on a Kovar feedthrough lead. The ion source assembly is mounted onto the Nylon insulating flange used also in conjunction with the duoplasmatron ion source, and negative ions are extracted by means of the same conical drawout electrode as that used with the duoplasmatron. Provisions were made for differential pumping of the space between the discharge source anode cylinder and the constrictor electrode. A 375 liter/min mechanical pump was employed. Although this arrangement allowed an increase in the usable gas flow, it was not found to improve the attainable ion currents.

Initially, the discharge was powered by means of microwave excitation. This mode of excitation has the advantage that it requires only a relatively low cathode potential. With oxygen as the discharged gas, ion intensities of 3×10^{-7} amps for both O^- and O_2^- were produced regularly. However, it was discovered that the ion beams thus generated were often modulated with a 120 Hz component. The source of this modulation was a ripple on the anode voltage of the microwave generating magnetron. Even though the ripple and the corresponding high frequency modulation amounted to only 1 percent, the ion beam sometimes was fully modulated. Additional complications arose from uncontrollable phase

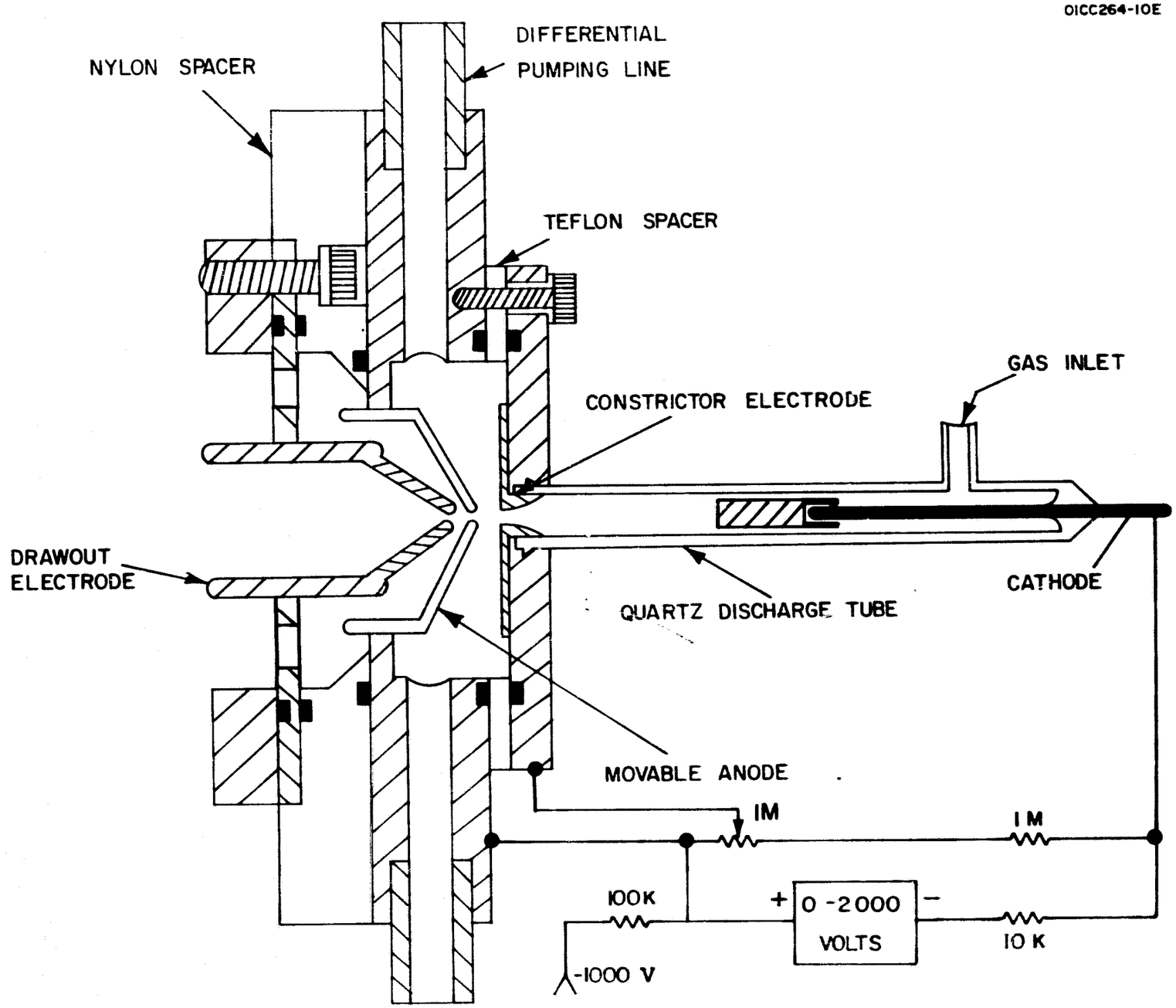

Figure 1. Cross section, discharge ion source.

shifts produced by interaction with other noise sources and from plasma oscillations triggered by the high frequency modulations. The magnitude of the effect upon the ion beam is probably caused by oscillations of the discharge striation from which the ions are withdrawn. Since the modulation amplitude could not be reduced by simple electric filtering devices, the concept of microwave excitation was abandoned and the glow discharge source was powered by a dc supply. For oxygen as the discharged gas a cathode voltage of 1000 volts was found sufficient, but hydrogen required cathode potentials up to 2000 volts to sustain the discharge at low pressures (~ 50 microns). At higher pressures the gas efflux became excessive and the ion intensity decreased.

C. Interaction Chamber

Differential pumping is employed to achieve the necessary low pressures in the individual sections of the apparatus. The ion accelerating region, the magnetic analyzer and the interaction chamber are each served by a diffusion pump of appropriate size. The first two pumps are fitted with water-cooled baffles, but the baffle serving the interaction chamber is cooled with a freon refrigeration system. Low interaction chamber pressures are required for photodetachment experiments because the detachment of electrons by ion-neutral collisions constitutes a noise source which must be kept small. In practice, dynamic pressures achieved in the interaction chamber were typically 2×10^{-7} torr, when the ion source was run with oxygen or air. While this pressure is higher than had been anticipated on account of gas flux estimates, it is sufficiently low for photodetachment experiments. It appears that in this pressure range outgassing from walls and O-rings, etc. is the most critical factor which could not be assessed accurately beforehand. Other undesirable sources of electrons were found to be produced by interaction of the ion beam with orifices and with the ion trap, and by the liberation of photoelectrons from the components in the interaction chamber. The reduction of these noise sources required several modifications of the design of the interaction chamber as given in a previous report. These will now be discussed.

The ion collector consists of a Faraday cage with tilted target area, so that secondary electrons are mainly reflected toward the inner walls of the cage rather than back into the interaction region. The collector was further shielded against external fields and a small negative potential was applied to prevent electrons from escaping the cage. Because of the emission of photoelectrons, the shield had to be removed (see below). Then the negative potential could no longer be applied without distorting the electron collector field. Accordingly, a different arrangement was required to keep secondary electrons out of the interaction region. Similarly, it was found that electrons formed at the mass

spectrometer exit orifice were propelled into the interaction region where they contributed to the background noise. This noise source also required elimination.

Preliminary experiments indicated a considerable background due to photoelectrons. The original design of the interaction chamber made use of a rear window for the escape of the radiation. The window was tilted to prevent the direct reflection of light back into the interaction region. Clearly, this arrangement increased the interaction of UV light with the walls of the chamber, thereby giving rise to an appreciable production of photoelectrons. To eliminate the back scattered light, the rear window was replaced by a Wood's horn. This modification did not, however, reduce the photoelectron signal by a sufficient amount.

A more prominent source of photoelectrons appeared to be scattered light falling onto the ion beam aperture cones. The aluminum cones were provided in the original design to limit the exposure of the ion beam to the background gas density in the chamber to a length of 1.5 cm. The cones served simultaneously as the mass analyzer exit orifice, and the ion collector shield, respectively. It was attempted to reduce the production of photoelectrons at the cones by coating them with platinum, since platinum reportedly has a high photoelectric work function (Ref. 7). However, the coating was found to increase the photoelectric effect rather than decrease it. A good cover of carbon black was much more effective in reducing the photoelectron signal, but the resulting noise level was still too high. As a consequence, the beam aperture cones were removed entirely, and they were replaced by a different arrangement.

The modified design is shown in Figures 2 and 3. The mass analyzer exit orifice was located further back toward the magnetic field. This modification did not change the location of the ion beam focal point; but to preserve intensity, the orifice was made slightly larger so that there occurred a loss in mass resolution. The lower resolution was tolerable in the experiments reported here. The new analyzer exit orifice and the Faraday cage serving as the ion beam collector were both shielded by plates with apertures sufficiently large to avoid any interaction with the ion beam. The shielding plates were connected to a negative potential with respect to ground, so that secondary electrons produced by interaction of the ion beam with the analyzer exit aperture and the ion collector were repelled. The two shielding plates were mounted onto a U-shaped band of steel which being on the same negative potential as the shielding plates, aided in driving electrons created inside the interaction region toward the electron multiplier detector. In addition, the shield of the electron multiplier focusing electrode was electrically insulated from its holder and was connected to the same negative potential supplied to the ion aperture shielding plates. As

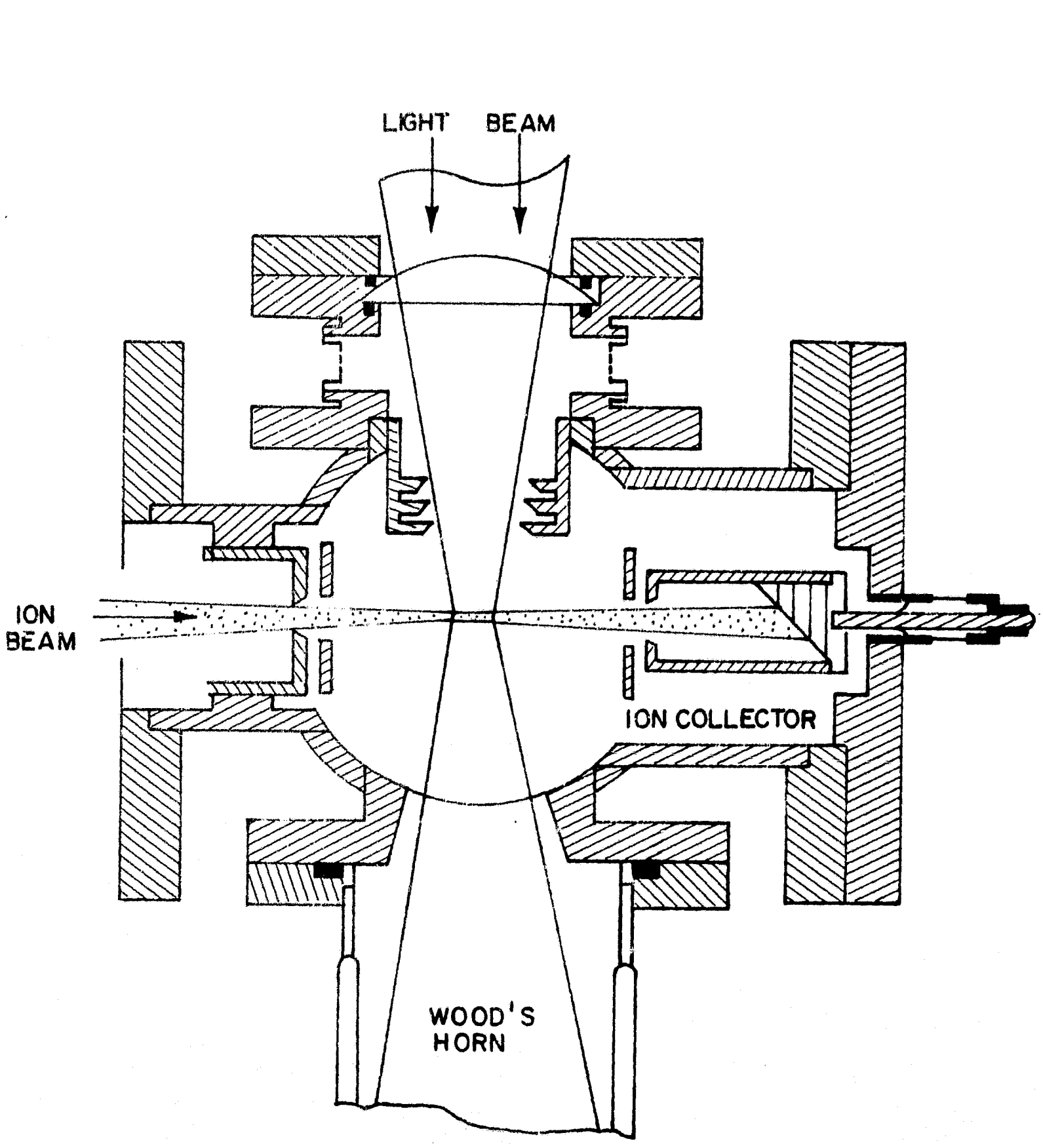

Figure 2. Sectional view, modified interaction chamber. Ion beam comes from left, light enters from top.

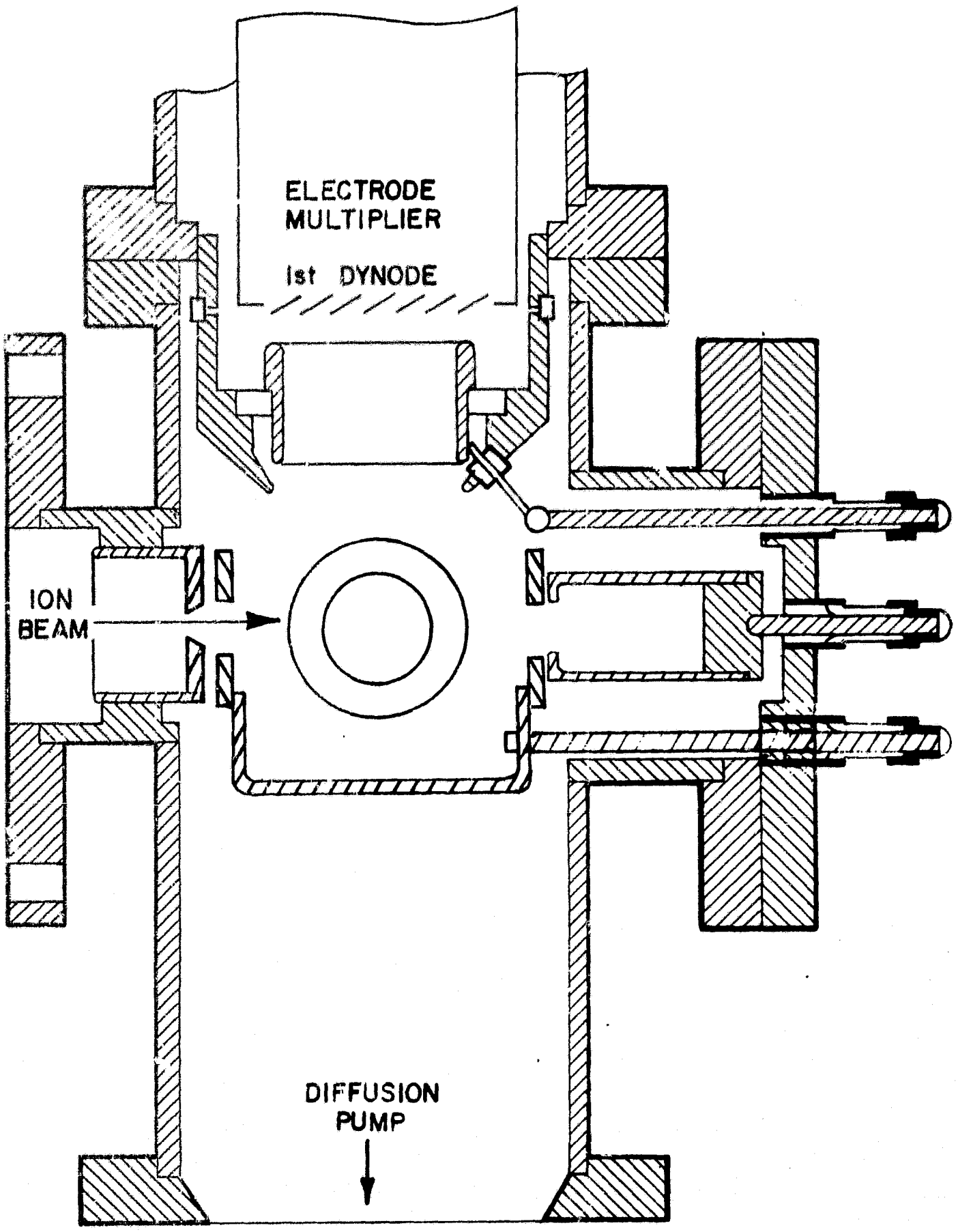

Figure 3. Sectional view, modified interaction chamber. Ion beam comes from left.

a result, a potential well was formed inside the interaction chamber such that electrons produced on the chamber walls were repelled, whereas all the electrons inside the well were pushed upwards and entered the electron multiplier detector.

After the implementation of the described modifications a small but significant photoelectron background signal persisted. Since the remaining photoelectron signal was proportional to the size of the light beam, it appeared that scattering of light by irregularities of the final focusing lens was responsible. A portion of the scattered light would fall on the inner sides of the ion aperture shielding plates. To reduce this contribution to the background noise, an optical aperture was installed between the focusing lens and the photodetachment region. The aperture was made sufficiently large to avoid contact with the main light beam converging to its focal point in the photodetachment region, but small enough to prevent most of the scattered light from reaching the ion beam shielding plates. The optical aperture was coated with an optical black; this reduced the background signal due to photoelectrons to a level which was negligible when the ion beam current was of the order of 10^{-7} amps and photodetachment cross sections were of the order of 10^{-18} cm^2. For smaller values of either photodetachment cross sections or ion currents, the photoelectron signal still presented a significant background. This background could be reduced further if light of wavelengths less than 2800Å was eliminated by means of a pyrex filter. Most of the measurements reported here were taken under these conditions.

Undoubtedly, the photoelectron signal can be improved further. One way is to enhance the monochromaticity of the light entering the ion chamber. It should be remembered that in the present arrangement the ion beam selects the effective wavelength range by its overlap with the spectrum produced in the focal plane of the light beam, and that a rather broad wavelength range enters the photodetachment chamber. The light entering the chamber could be made more monochromatic by the insertion of a monochromator exit slit and refocusing elements outside the photodetachment chamber. There would still remain the scattering of light by the focal lenses, and these would have to be improved.

D. Additional Experimental Details

The addition of a Wood's horn in the rear of the photodetachment chamber no longer permitted the monitoring of the optical spectrum by a photoelectric sensor during the photodetachment experiment. Intercepting the light beam before it entered the photodetachment chamber would not provide a representative spectral intensity distribution, because at that point the radiation was not yet focused. Fortunately,

it was found that once the light source had stabilized, the intensity distribution of the emitted spectrum remained essentially constant. Stable operating conditions were obtained about 30 minutes after start-up, and the relative spectral intensity distribution did not change noticeably after repeated shut-down and start-up cycles. It was possible, therefore, to determine the relative spectral intensity distribution in the center of the photodetachment chamber by separate experiments. For this purpose, the system was vented before and after a series of photodetachment experiments, and an auxiliary slit was placed at the location of the ion beam-light beam crossing inside the photodetachment chamber. The Wood's horn was taken off and replaced by an Eppley thermopile. The width of the auxiliary slit was adjusted to resemble the effective width of the ion beam, and a spectrum was taken. Since the response of the thermopile is proportional to the power received, the number of photons passing through the auxiliary slit in the corresponding wavelength band can be calculated. Figure 4 shows a typical spectral intensity distribution thus obtained. It should be noted that the spectrum emitted by the light source consists of strong lines superimposed on a weaker continuum. This is not evident in Figure 4 because of the insufficient spectral resolution. For comparison, Figure 5 shows the spectrum (not the intensity distribution) at much higher spectral resolution, as given by the manufacturer of the light source.

The spectral resolution attainable in the present experiments depends on the width of the entrance slit of the monochromator, the width of the ion beam at the point of interaction, on the quality of optical focusing, and on the monochromator grating. In the experiments, the entrance slit width was kept constant at 0.2 cm. The grating had 1200 lines/mm (and was blazed for 3000Å). For these conditions, the predicted half width resolution bandpass is about 230Å, if the focal length of the exit lens equals that of the entrance lens, and if the ion beam width is 0.2 cm. Although the initial measurements gave a spectral resolution in agreement with expectation, it was found that the ion beams had width less than 0.2 cm diameter. Probings of the ion beam showed that its width was 0.15 cm for O^- ions, with a spread of about one half of a degree. O_2^- ion beams had a similar size, but the beam width of NO_2^- was larger by about 15 percent. The fact that the ion beam widths were less than anticipated made it possible to improve the spectral resolution. The entrance slit width was kept constant at 0.2 cm, but the flat mirror directing the dispersed radiation into the photodetachment chamber was replaced by the spherical mirror of 50 cm focal length originally provided for this task. The optimum spectral resolution at half width then became 180Å.

The somewhat unexpected result that ion beam widths could vary with the type of ion made it necessary to determine the spectral intensity distribution with respect to the effective width of the ion beam. For this, it was not necessary to measure the size of the ion beam, since the effective width was apparent from the response of the

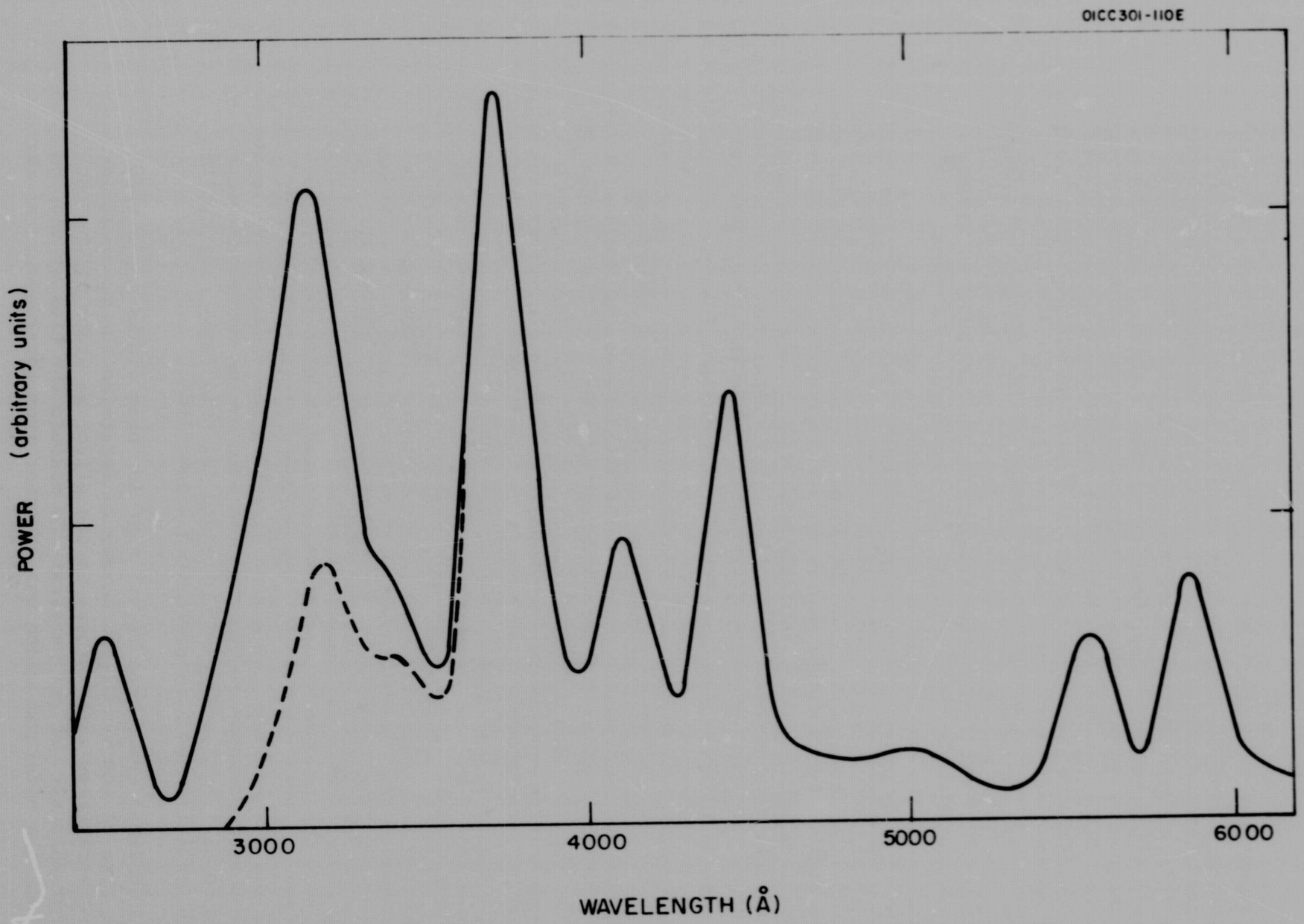

Figure 4. Thermopile response of monochromator scan, spectral resolution 180Å half width. Solid line: without filter, broken line: with Pyrex filter.

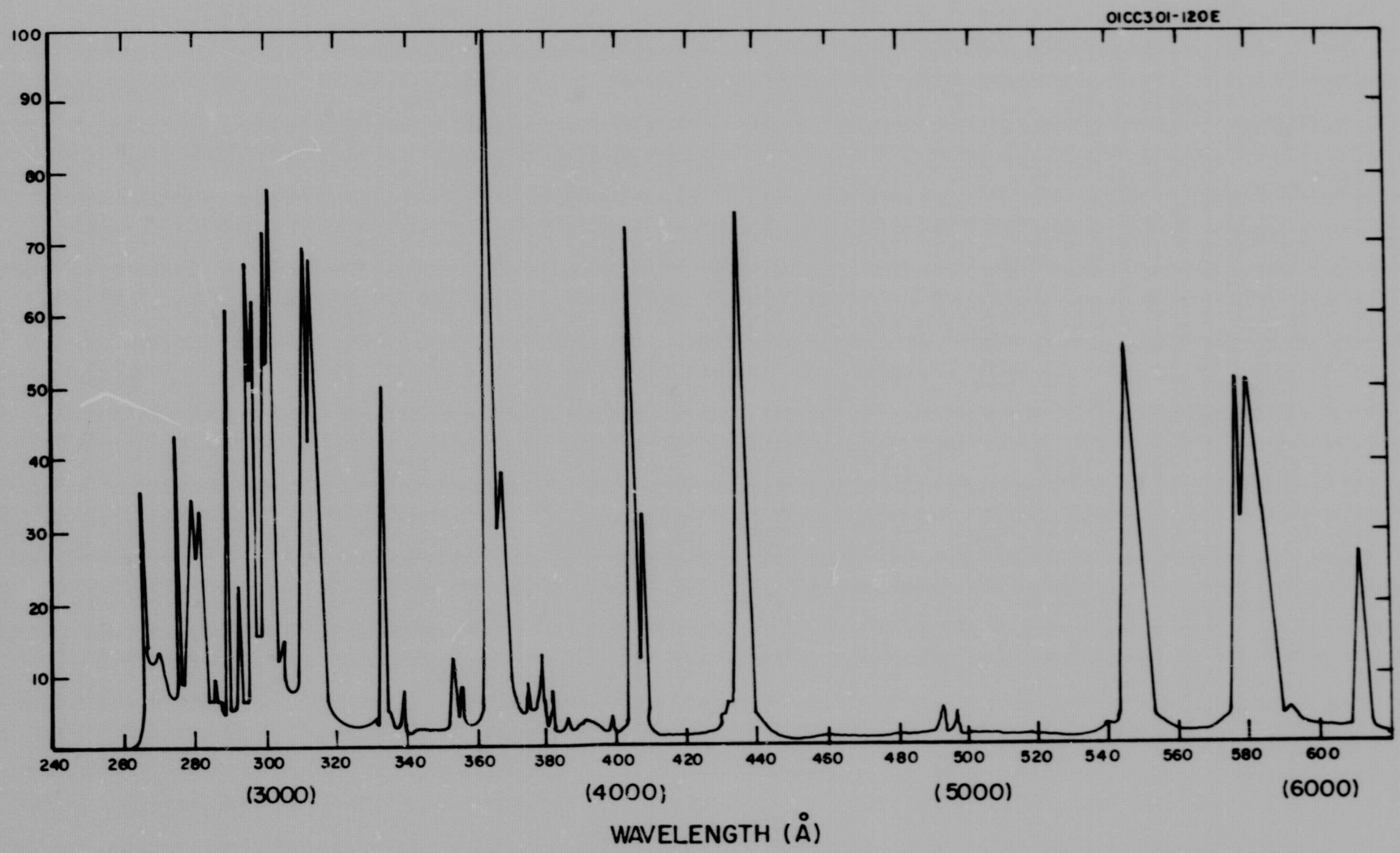

Figure 5. Spectrum of mercury-xenon arc source as given by manufacturer. Spectral resolution ~2Å.

photodetachment current when scanning across the central image of the monochromator, i.e., the undispersed, directly reflected light beam. Therefore, in measuring the spectral intensity distribution, the width of the auxiliary slit was adjusted such that the half width of the central image measured with the thermopile was the same as that observed in the photodetachment experiment. It is clear that this procedure would give faulty results, if the ion beam density were not sufficiently uniform, but then the shapes of the central images observed in both experiments should be rather different. The observations show, however, that in all cases the shapes are similar, and that deviations cannot be detected. Figure 6 shows an example for an O^- ion beam. The conclusion is that the generated ion beams are reasonably homogeneous, and that their effective width can be represented by a slit of similar width.

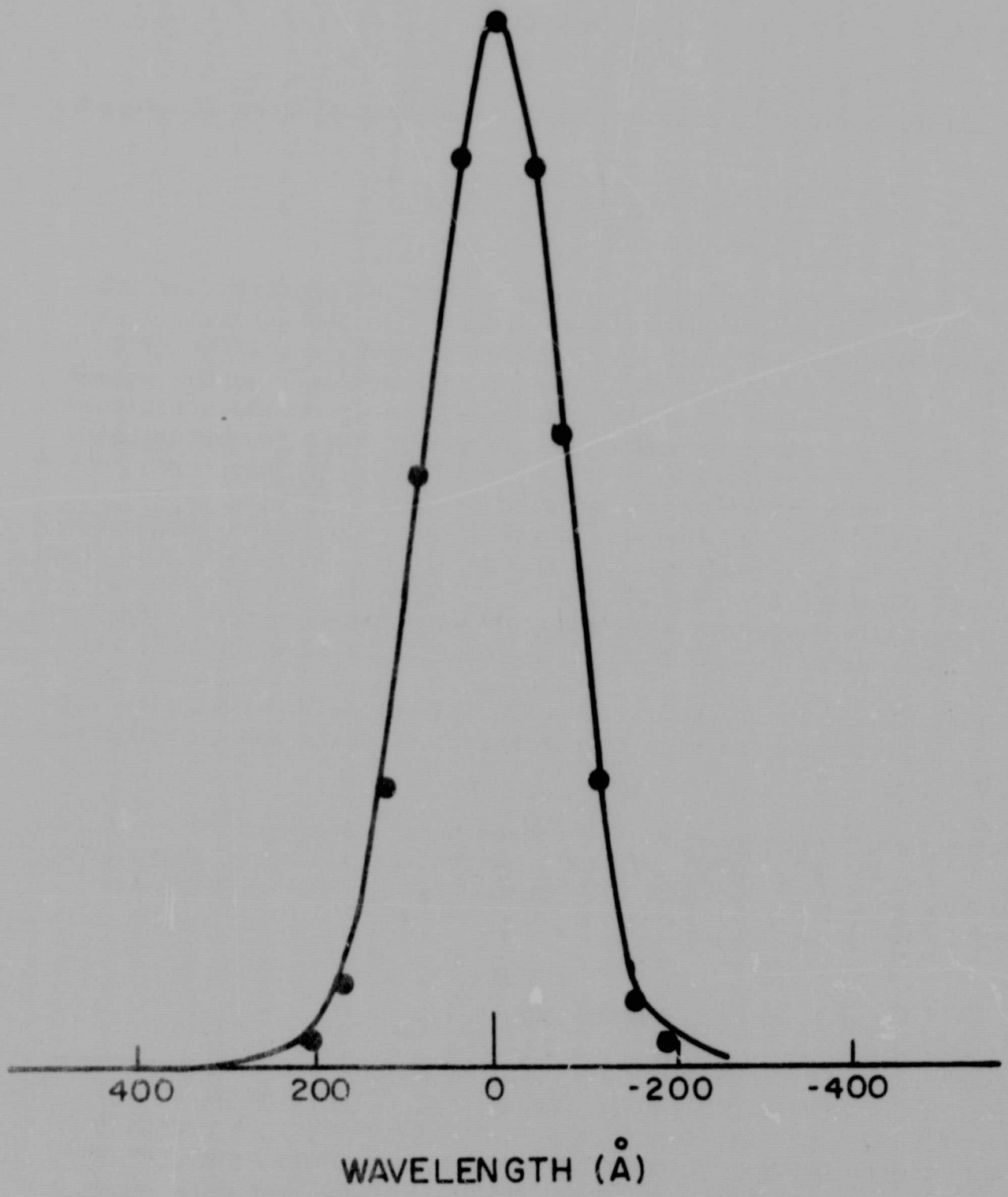

Figure 6. Comparison of central image profiles. Solid line: Photodetachment signal, determined by width of ion beam. Points: Normalized thermopile response determined by auxiliary slit in place of ion beam, adjusted to same half width resolution (180Å).

III. RESULTS

The signal observed due to the photodetachment process is given by

$$S = kj_e = kj_i \sigma I/v_i \ell$$

where k is an apparatus constant, j_e and j_i are the electron and ion currents respectively, I is the light intensity in photons/sec, σ the photodetachment cross section, v_i the speed of ions, and ℓ the effective width of the ion beam at the point of interaction. In the present experiment, the apparatus constant k depended mainly on the efficiency and the gain of the electron multiplier detector. Due to variations from day to day, it was difficult to determine these factors precisely, so that the determination of absolute cross section values was not attempted. Hence, the wavelength dependence of the photodetachment cross section was measured, and the absolute magnitude of the cross sections was obtained by comparison with a standard. The O^- ion was used as a suitable reference standard. O^- was preferred to H^- (for which the cross sections are known from theory), because the data obtained for O^- were more reliable than those for H^- due to ion current fluctuations and noise in the latter case. Absolute cross section values for O^- photodetachment have been reported by Smith and by Branscomb et al. (Ref. 9).

In the present experiments, photodetachment data were obtained for the ions: O^-, H^-, NO_2^-, O_2^-, and OH^-. Attempts to observe photodetachment for the ions NO_3^- and CO_3^- were unsuccessful. The results are described below.

A. Atomic Oxygen Ion

Photodetachment cross sections obtained for O^- are shown in Figure 7 as a function of wavelength and in Figure 8 as a function of energy. The O^- photodetachment threshold occurs at 1.465 eV energy, corresponding to the wavelength 8460Å. This is beyond the wavelength range covered by the present experiments which went only to 6200Å. The data shown were obtained with a half width spectral resolution of 180Å, as given by the width of the central image. The signals were recorded at a scan speed of 200Å/min, and the recorder traces were evaluated at 50Å intervals. Although this is less than justified by the spectral resolution, the data points thus obtained indicate better the involved scatter of experimental values. An average spread of about $\pm$ 10 percent is evident

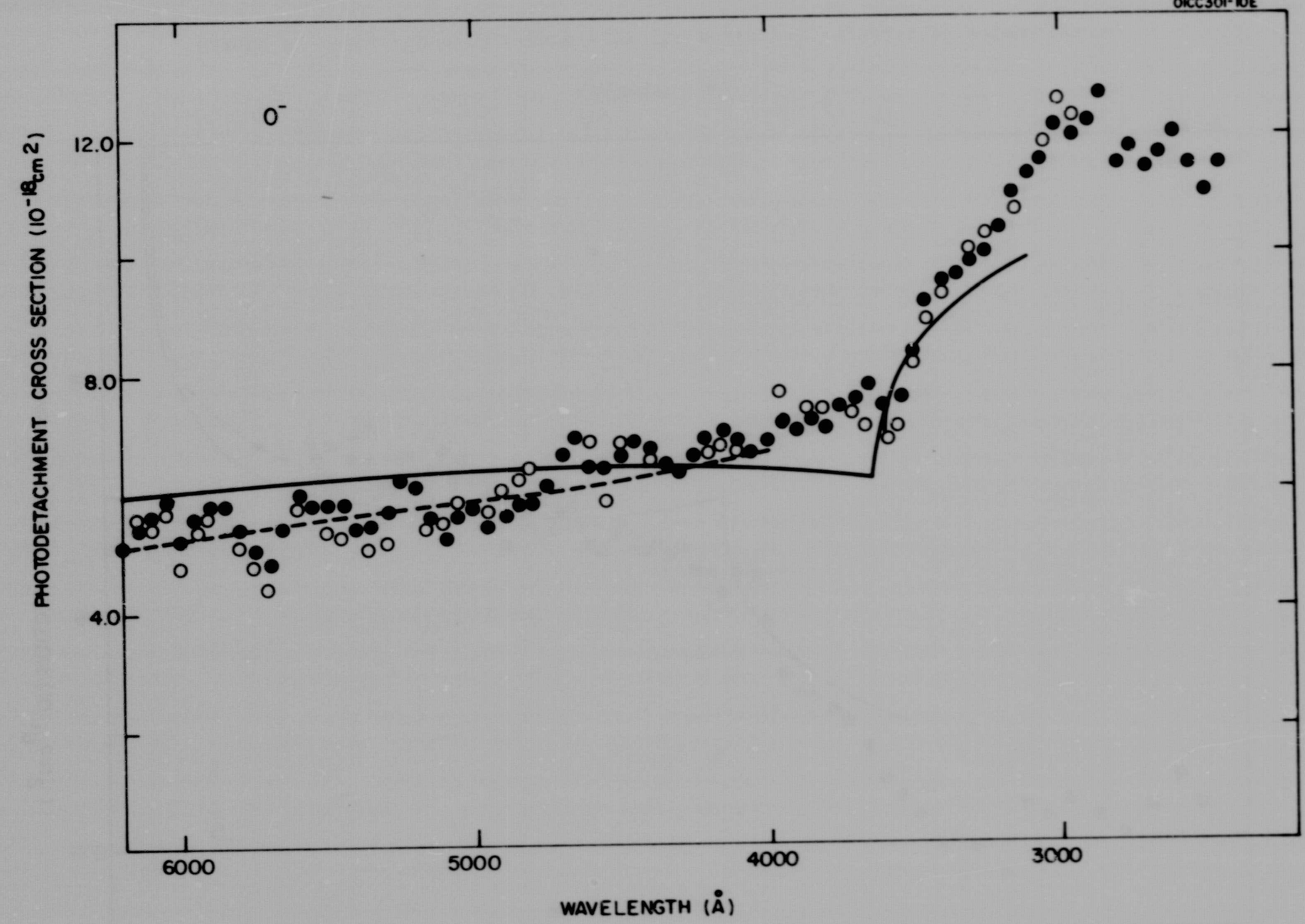

Figure 7. Photodetachment cross sections for O^-. Filled points, without filter; Open points, with Pyrex filter. Spectral resolution 180Å half width; Solid line, interpolated data of Branscomb, et al.(Ref.8); broken line, interpolated data by Branscomb, Burch, et al. (Ref. 9).

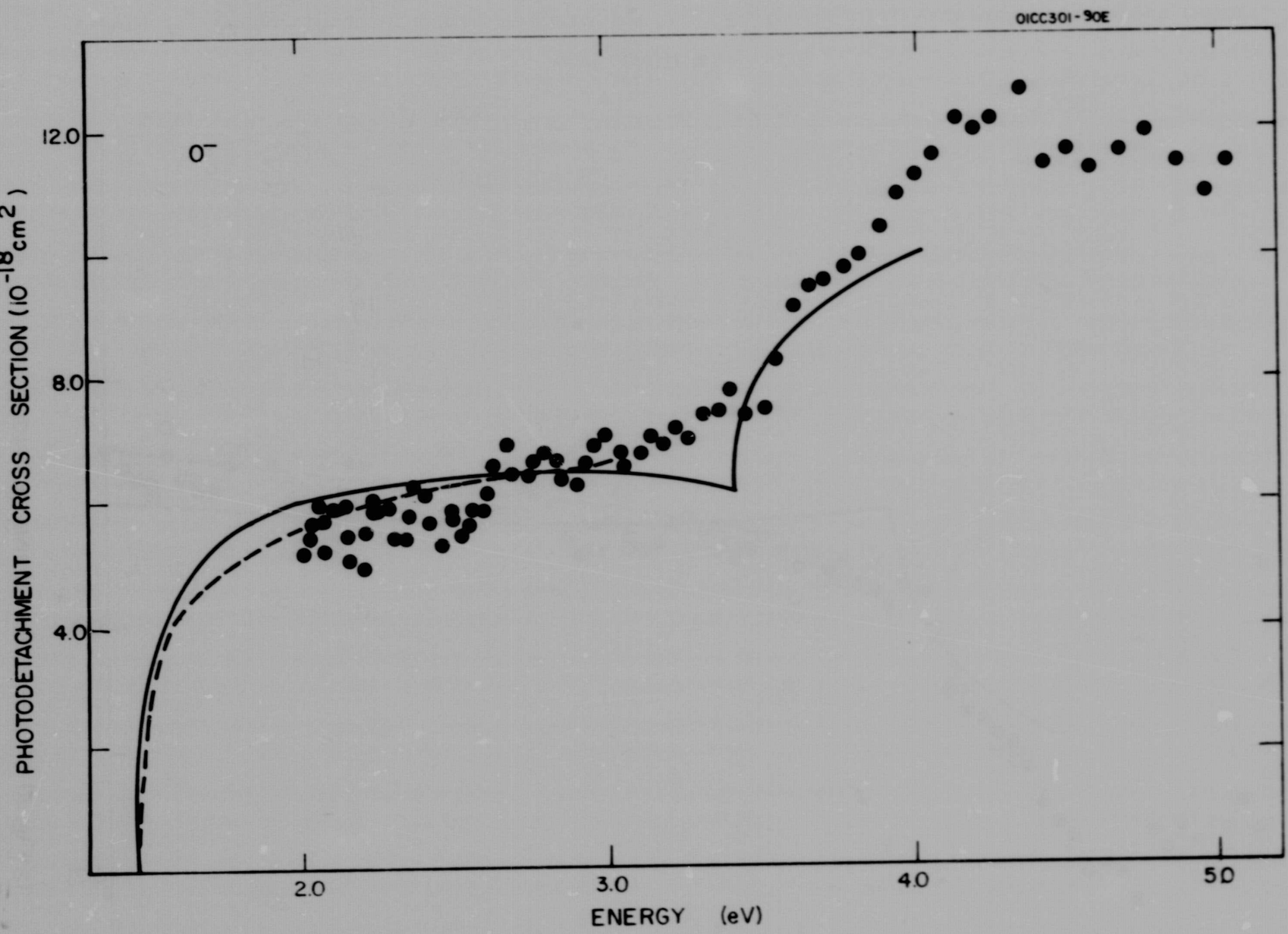

Figure 8. Data shown in Figure 7 by the solid points, plotted versus energy.

from the figures. Data were obtained with and without a pyrex filter in the optical path. In the first case the spectrum below 3000Å is eliminated, and any interference produced by the second order spectrum of light in the 2500 to 3000Å wavelength region with light in the 5000 to 6000Å wavelength region is also eliminated. The good agreement of the data obtained with and without the pyrex filter in the wavelength region 5000 to 6000Å indicates, that the contribution of second order radiation is ngeligible. The solid lines shown in Figures 7 and 8 indicate the data obtained by Branscomb, Smith and Tisone (Ref. 8) with a spectral resolution of 100Å, the dashed lines indicate the earlier data which Branscomb, Burch, Smith and Geltman (Ref. 9) had obtained using filters of about 500Å resolutions. It can be seen that the present data fit better to the latter results, both showing a slight slope. Hence, the present data were fitted to those reported by Branscomb, Burch, Smith and Geltman in the wavelength region 4000 to 6000Å, to give the absolute photodetachment cross section shown. The reason for the difference in the previous results has as yet not been clarified. The spectral resolution in the present experiments is comparable to that available to Branscomb, Burch, Smith and Geltman (Ref. 10), whereas the more recent data (Ref. 9) by this group have achieved a five-fold improvement. However, the variation of the cross section with wavelength is too small (even at the lower resolution) to be much influenced by the five-fold difference in the spectral resolution.

The rise in the cross section observed at wavelengths below 3600Å is due to the process

$$O^- (^2D) + h\nu \rightarrow O (^1D) + e$$

yielding an excited oxygen atom and occurring in addition to the process giving oxygen atoms in the ground state. The present data do not define the visual threshold for $O(^1D)$ formation as well as those by Branscomb, Smith and Tisone (Ref. 8). The slopes of the cross section curve obtained in the present work intersect at 3640Å, corresponding to 3.41 eV, whereas the above authors give 3.432 eV for the threshold. The agreement is reasonable. The rate of increase of the cross section values at wavelengths below the $O (^1D)$ threshold is similar to that reported by Branscomb et al. They point out that it is not as great as predicted on theoretical grounds. The present photodetachment cross section results sustain that observation. At wavelengths shorter than 3000Å the cross section curve levels off, and according to the present data actually decreases. In this wavelength region the present data are much less reliable than at longer wavelength, due to the presence of a background due to photoelectrons, as described in the previous section.

In deriving photodetachment cross sections, the background was deducted. It is already present at 3300Å, increases toward shorter wavelengths, and maximizes at 2900Å. At 3000Å, it constitutes about one half of the total signal recorded, yet when taken into account, the derived photodetachment cross sections are in good agreement with those obtained with the pyrex filter which essentially eliminates the photoelectron signal. Accordingly, it is felt that the photodetachment cross sections deduced for O^- in the 2500 to 3000Å provide a realistic representation of the true cross section values.

B. Atomic Hydrogen Ion

The experimental and theoretical work on the photodetachment of H^- has been reviewed in detail by Branscomb (Ref. 10). It has been shown that the photodetachment cross sections observed are in good agreement with theory if the latter is based on the dipole velocity matrix elements representation. The theoretical results obtained by John (Ref. 11), who solved numerically the Hartree-Fock exchange equations for the electron in the atomic hydrogen field, and those of Geltmand and Krauss (Ref. 12) who used a variational free state treatment, are practically identical. A divergence of about 12 percent exists between the theoretical and experimental results in the wavelength region above 10,000Å. In the spectral region covered here, 3000 to 6200Å, the experimental data should fit the theoretical curve very closely. The cross section data reported by Smith and Burch (Ref. 13), normalized to the integrated H^- absorption coefficient of Branscomb and Smith (Ref. 14), coincide well with theory, but they cover only the wavelength range above 4000Å. It was, therefore, of interest to extend the measurement of H^- photodetachment cross sections to lower wavelength.

The present results for H^- are shown in Figure 9 as a function of wavelength. At wavelengths above 4600Å the data exhibit considerable scatter due to several experimental factors: (a) the excellent mass resolution achieved with the magnetic analyzer made the transmitted ion current of H^- exceptionally susceptable to slight perturbations of the discharge operating conditions on the origin (and thus the initial velocity) of H^- ions; (b) the total H^- ion current obtained was only 3×10^{-8} amperes due to the particular source operating conditions, which for H^- were not as favorable as for other ions; (c) the pressure in the photodetachment chamber was about three times higher when the apparatus was run with hydrogen than for other gases; and (d) the light intensity available in the 4600 to 5500Å wavelength region is weaker than that below 4600Å, so that the effect of the various noise sources upon the measurements is more pronounced. Due to these problems, three sets of data were gathered in consecutive runs and were averaged. Although this procedure reduced the error somewhat, it is evident from Figure 10 that in the 4600 to 5800Å wavelength region the experimental scatter persists.

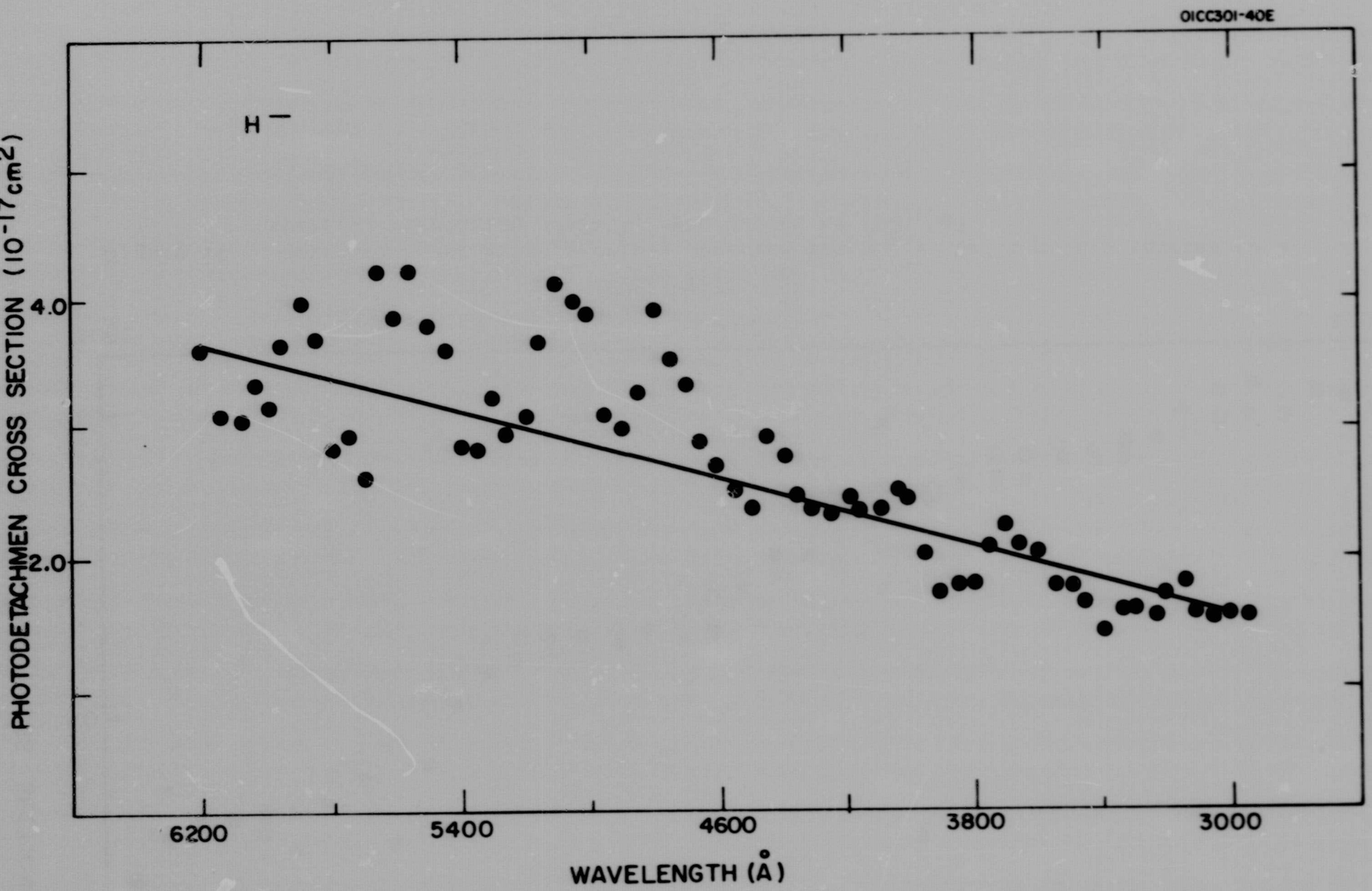

Figure 9. Photodetachment cross sections of H^- versus wavelength, obtained by using O^- as a standard. Spectral resolution 210Å half width, solid line refers to theory.

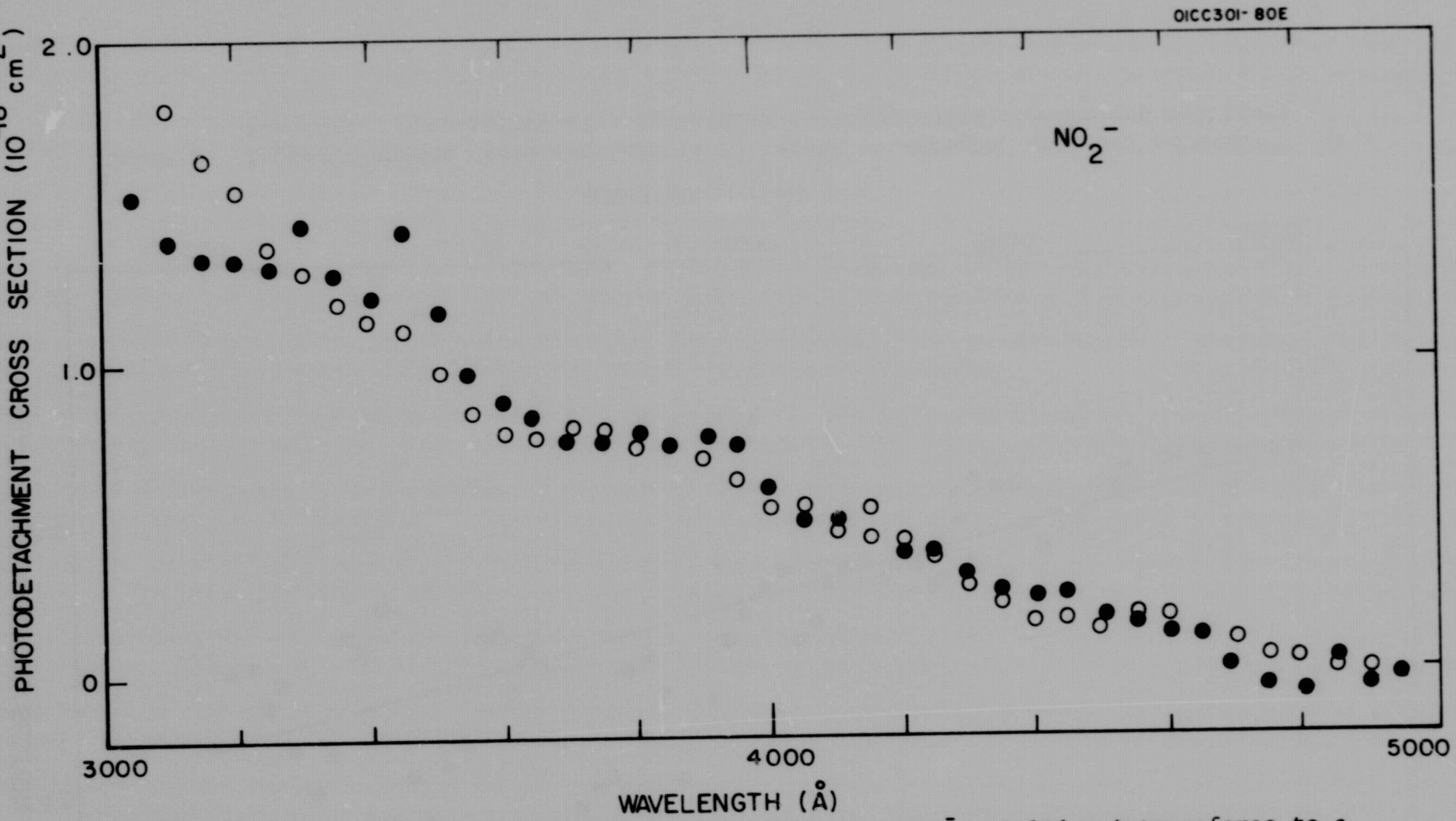

Figure 10. Photodetachment cross sections observed fro NO_2^-. Solid points referes to a spectral resolution of 240Å, open points to 200Å half width.

The data for H^- were normalized to those for O^- discussed in the previous section. The absolute photodetachment cross sections thus obtained for the H^- ion are in reasonable agreement with the theoretical cross section curve which in Figure 9 is represented as a solid line. In the wavelength regions 5800 to 6200Å and below 4600Å, where the scatter of the data points is not excessive, the experimental cross sections agree with the theoretical ones within an error of less than 15 percent. While the accuracy thereby achieved is not as high as that obtained by Burch and Smith (Ref. 13), it is clear that the present data show that the cross sections for H^- extend toward shorter wavelength as predicted by theory, and that the absolute values, compared to O^-, coincide well with those given by Branscomb and coworkers. Conversely, since the cross sections for photodetachment of H^- are the only ones accurately accessible by theory, the good agreement of the present measurements for H^- with the theoretical curve in the 3000 to 4600Å wavelength region provides additional confidence to accept the photodetachment cross sections derived for O^- as a standard against which data for other ions can be compared.

C. Nitrite Ion

Photodetachment of NO_2^- was observed in the present experiments at wavelengths less than 4750Å. Earlier attempts to photodetach NO_2^- by Branscomb and collaborators (Ref. 15) were limited to the wavelength region greater than 4100Å, where the NO_2^- photodetachment probability is low. Nevertheless, weak signals were observed which indicated a threshold at about 2.5 eV energy. The present experiments have confirmed the reality of the earlier data. The photodetachment cross sections measured for NO_2^- are shown in Figure 10 as a function of wavelengths. The data represented by the filled circles were obtained from NO_2^- produced by operating the discharge ion source with a mixture of air and oxygen. The ion current was 8×10^{-8} amps and the spectral resolution about 240Å at half width. The open circles were obtained by operating the ion source with a mixture of NO_2 and oxygen. In this case the ion current was 4.5×10^{-8} amps and the achieved spectral resolution was 200Å at halfwidth. Except at the short wavelength end, the data points overlap each other well, indicating that they are internally consistent.

As shown in Figure 10, photodetachment from NO_2^- becomes distinguishable from the background noise at 4700Å. Toward shorter wavelengths the cross section rises to a plateau at about 4000Å. A further rise commences at 3600Å until the cross section reaches a value of $1.6 \pm 0.2 \times 10^{-18}$ cm^2 at 3100Å. The precise location of the onset of photodetachment is masked by the noise level, but from an extrapolation

one derives the onset wavelength 4780 ± 80Å. Correction for the instrumental resolution gives the apparent photodetachment threshold 4560 ± 80Å, which corresponds to an energy of 2.72 ± 0.04 eV. These values are consistent with the results quoted by Branscomb (Ref. 15) for wavelengths greater than 4250Å. However, the present cross sections in the overlapping wavelength region are higher by a factor of about five.

The derived threshold energy provides only a lower limit to the vertical photodetachment energy, because a portion of the NO_2^- ions are vibrationally excited. Subsequent to the formation of a negative ion in the discharge the ion drifts toward the anode, picking up energy in the electric field and losing energy by collisions. This mechanism leads to a quasi-Boltzmann vibrational energy distribution among the ions equivalent to a temperature estimated to be several thousand degrees. The excess vibrational energy cannot be radiated away because the radiative lifetime of the involved states is about two orders of magnitude greater than the transit time of the ions in the apparatus ($\sim 10^{-5}$sec). The problem of vibrational excitation exists also in the determination of ionization potentials by photoionizing neutral molecules, despite the much lower temperatures. Watanabe (Ref. 16) has shown that a semi-logarithmic plot of photoionization cross sections versus energy often indicates the beginning photoionization of ground-state molecules, as compared to that of vibrationally excited ones, by a break in the cross section curve. A similar procedure is appropriate in the case of photodetachment. Its application to the present data is shown in Figure 11. The initial linear rise of the cross section has a slope corresponding to a vibrational temperature of NO_2^- of 3000°K, which is in accord with expectation. A break in the curve occurs at 3.10 ± 0.05 eV. Due to the limited spectral resolution amounting to several tenths of an electron volt in the spread of photoenergy, the break is not sharp, so that the precise location of the change in slope of the curve is uncertain by about 0.05 eV. The fact that it coincides with the edge of the plateau makes it likely that the break corresponds to the transition between the NO_2^- and NO_2 ground states. In the vicinity of the break the plateau has a negligible slope. This would imply a minimal change in the internuclear distance during the transition. For if the upper and lower potential curves were considerably displaced, the variation in the Franck-Condon factors would produce a variation of the photodetachment cross sections of the individual transitions, and since these cannot be resolved, the cross section curve would have to exhibit a slope. However, the data in Figure 11 admit the possibility that the plateau is an apparent one, forming the limb of the rising cross section curve at higher photons energies with a corresponding extension of that slope toward the break at 3.1 eV. Thus, the evidence for a negligible change in internuclear distance during the transition from NO_2^- to NO_2 is not unique and additional investigations are required to determine whether the NO_2^- and NO_2 ground states are in fact similar.

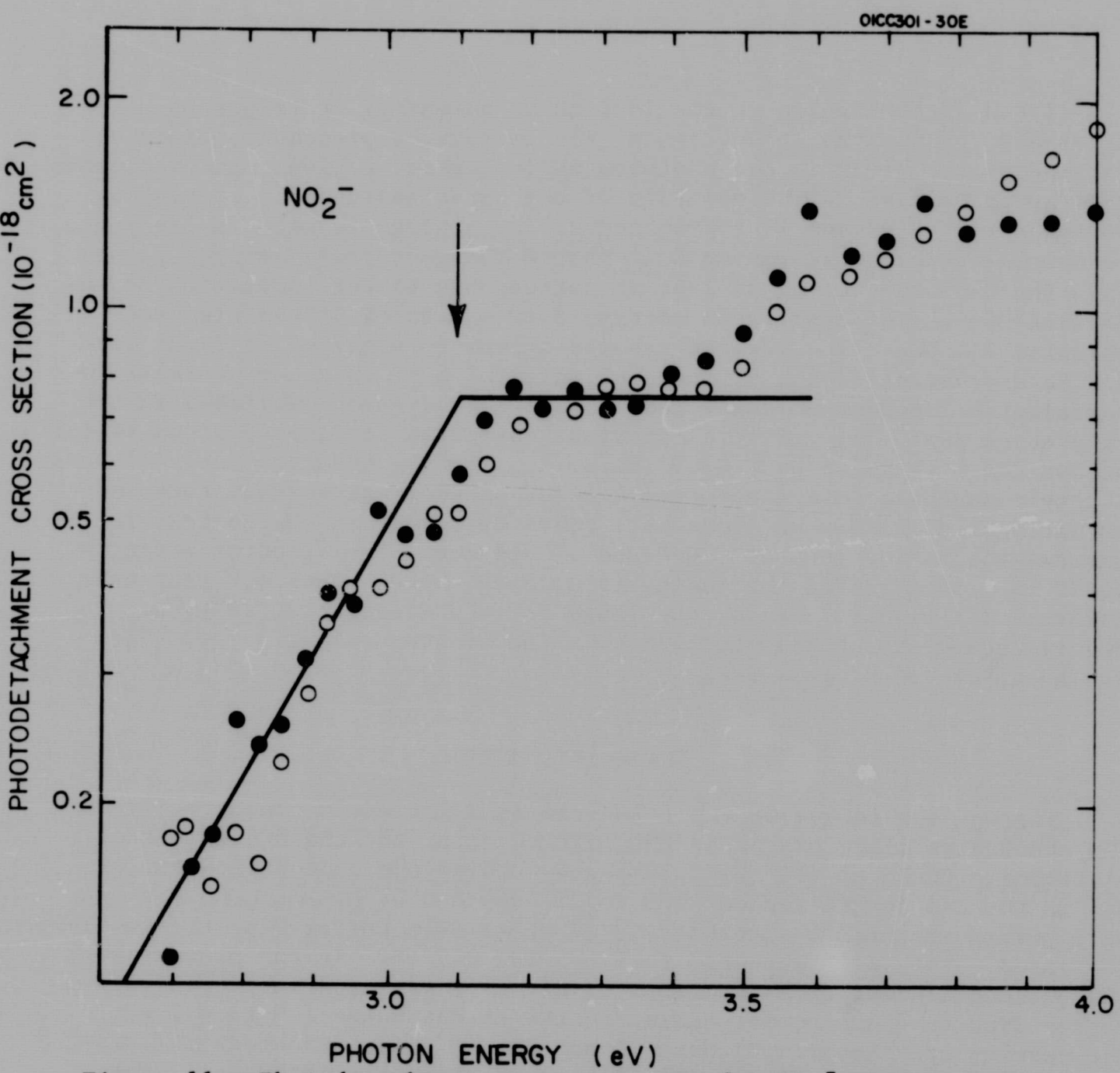

Figure 11. Photodetachment cross sections for NO_2^- plotted semi-logarithmically versus energy, to show break in the curve of 3.1 eV.

For a determination of the ionization potential it is not usually necessary to know the structures of the two states precisely, since the first distinct break in the photoionization cross section curve indicates the 0-0 transition in the majority of the cases and the higher members in the series are much less pronounced. By analogy it seems appropriate to associate the break in the NO_2^- photodetachment cross section curve with the 0-0 transition, so that it corresponds to the ionization potential of NO_2^-. The associated energy, 3.10 $\pm$ 0.05 eV is the electron affinity for NO_2. The present results appear to provide the first direct determination of the electron affinity of NO_2. Because of their importance, an account of these results has already been published in the literature (Ref. 17). Several previous estimates for the electron affinity of NO_2 range from 1.6 to 4.0 eV (Refs. 15, 18-20). Paulson (Ref. 21) has recently narrowed this range from a study of charge transfer processes to nitrogen dioxide. HS^- ions were found to result in charge transfer whereas the halide ions Cl^-, Br^- and I^- did not. The electron affinity of SH is 2.50 eV, that the iodine is 3.18 eV. The values for the other halogens lie higher. Hence, the range for the electron affinity of NO_2 is thought to be 2.50 to 3.18 eV. The present value, 3.1 eV, lies at the upper end of this range.

D. Molecular Oxygen

The O_2^- ion is one of the principal ions formed in the D-region of the atmosphere since oxygen is the main receptor for the attachment of electrons. Burch et al. (Ref. 22) have studied the photodetachment of O_2^- in the wavelength region 4000 to 25,000Å and by interpolation of the data points obtained a smoothly rising cross section curve as the wavelength decreased. The onset appeared to lie below 0.5 eV. In the present work the photodetachment cross sections of O_2^- were measured in the wavelength region 2900 to 6200Å corresponding to the energy range 2.0 to 4.2 eV. The results are shown in Figures 12 and 13. O_2^- was produced in a discharge of pure oxygen at ion intensities of about 5×10^{-8} amps. The spectral resolution was 180Å at half height. In the wavelength region 4000 to 6000Å, the data points coincide with the interpolated photodetachment cross section data of Burch et al. shown as a solid line. At shorter wavelengths the present data extend that curve towards higher cross section values, reaching 6×10^{-18} cm^2 near 2900Å.

In the energy region covered the states of neutral O_2 that can be reached by ionizing transitions from O_2^-, are the O_2 ($X^3\Sigma_g^-$) ground state and the excited states a $^1\Delta_g$ and $b^1\Sigma_g^+$. Taking the electron affinity of O_2 to be 0.43 eV (Ref. 23), the photodetachment thresholds corresponding to the three states are 0.43, 1.41 and 2.06 eV, respectively. It is doubtful, whether these thresholds can be made apparent in photodetachment experiments, because the internuclear distance of O_2^- is larger than that of the three O_2 states (Ref. 24), so that the

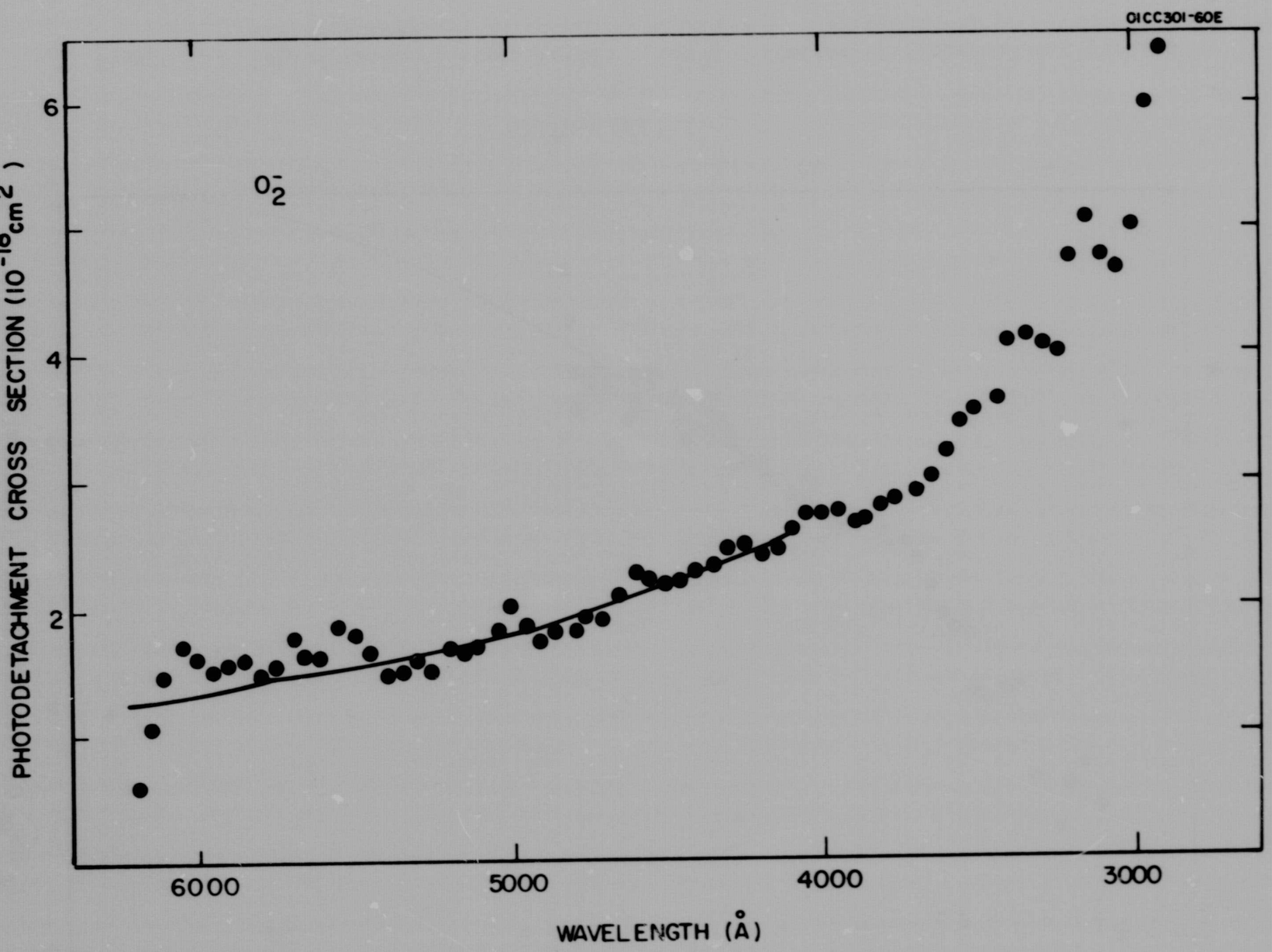

Figure 12. Photodetachment cross sections for O_2^- spectral resolution 180Å half width. Solid line shows interpolated data by Burch et al. (Ref. 22).

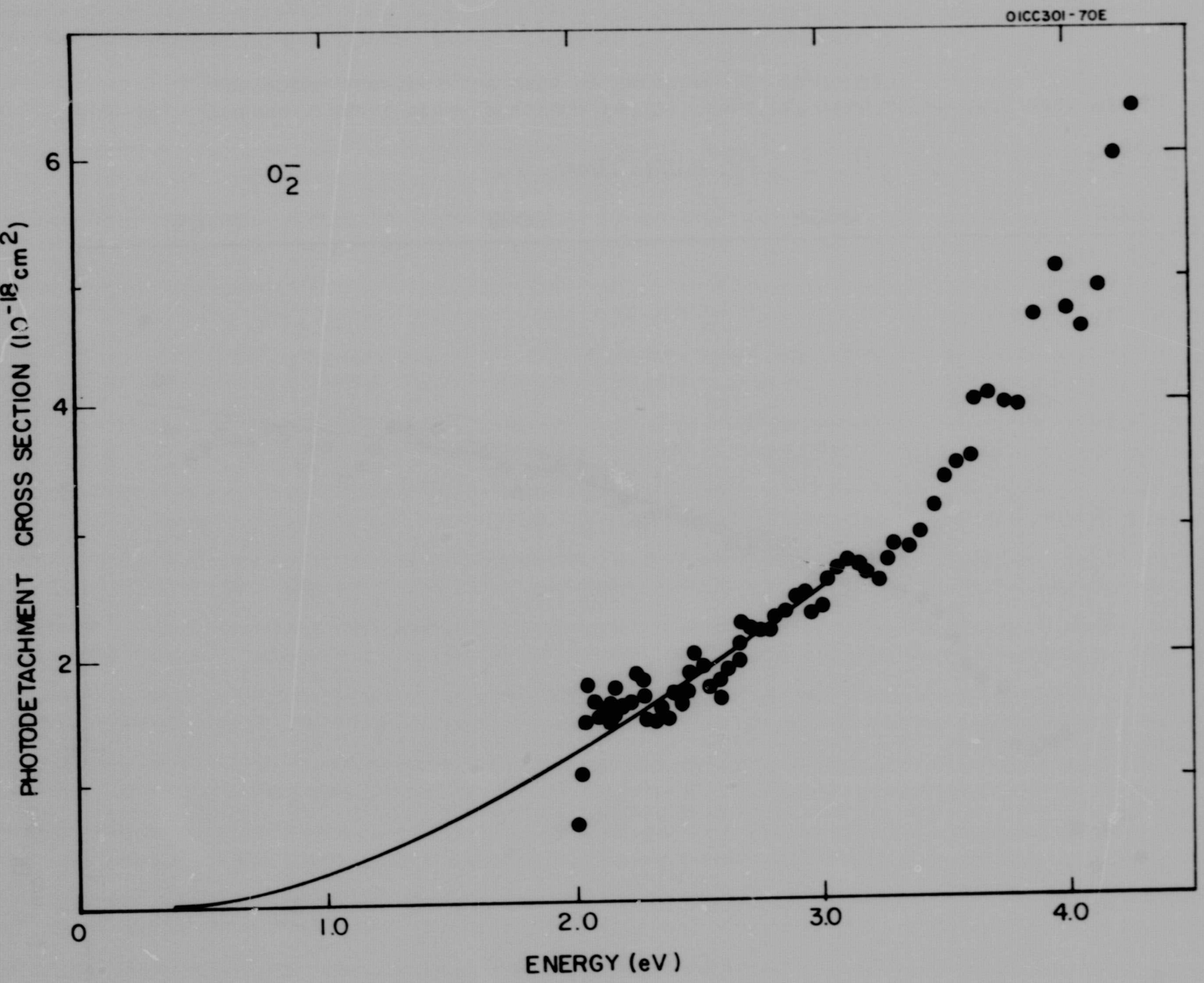

Figure 13. Photodetachment cross sections for O_2^- similar to Figure 12 but plotted versus energy.

0-0 transitions are disfavored in comparison with vertical transitions toward higher vibrational levels. In Figures 12 and 13, the data points in the vicinity of 6100Å (2.05 eV) appear to indicate a sudden rise in cross section which coincides with the expected onset of photodetachment to the $b^1\Sigma_g^+$ state. For the above reasons, however, these data points are to be viewed with caution, even though they deviate appreciably from the range of experimental scatter evidenced at shorter wavelengths (higher energies). Further experiments are evidently required to clarify this point.

Up to about 3 eV energy the rise of the cross sections with decreasing wavelength (increasing energy) is in accord with expectation. Since the bottom of the O_2^- potential curve is displaced by about 0.1Å from the equilibrium positions of the potential curves of the O_2 states (Ref. 24), the Franck-Condon probabilities should increase as higher vibrational levels of the various O_2 states become accessible. The individual vibrational level would not be resolved in the present experiments, particularly if the O_2^- ion is vibrationally excited. Since the vertical transition to the $b^1\Sigma_g^+$ state requires only about 3 eV, one would eventually expect decreasing Franck-Condon probabilities as the energy is increased further. Figure 13 shows, however, that the photodetachment cross sections above 3 eV, still increase considerably. This behavior must be associated with an increase in the electric transition moment. A contribution from autoionizing transitions can be practically excluded. Calculations by J. C. Browne (Ref. 25) indicate that the next excited state of O_2^-, designated $2\Pi_u$, is essentially repulsive. Accordingly, the transition O_2^- ($^2\Pi_g \rightarrow {}^2\Pi_u$) would lead to the dissociation products $O^- + O$. These could not be observed in the present apparatus. Since the $^2\Pi_u$ state is not bound, autoionization must be negligible. It is of interest to note, however, that if O_2^- is an abundant ion in the D-region during the daytime, the $^2\Pi_g - {}^2\Pi_u$ photodissociation process may have significance. Clearly, this process should be explored.

E. Hydroxyl Ion

The photodetachment of OH^- has been previously investigated by Branscomb (Ref. 26) and by Branscomb and Smith (Ref. 27). The photodetachment threshold lies at 1.78 eV energy, or about 7000Å. The present results on OH^-, although not covering the threshold region, are in good agreement with the previous data in the range of overlap. The results obtained in this work are shown in Figures 14 and 15 and by the indicated points, whereas Branscomb's results are shown as the solid curve which interpolates his data points. The wavelength dependence of the OH^- photodetachment cross section is characterized by a maximum achieved rapidly after passage of the threshold, and a gradual decline at wavelengths down to about 4000Å, where Branscomb's data terminate. The present results show that at lower wavelengths this trend continues at wavelengths down to 3400Å, but that at still shorter

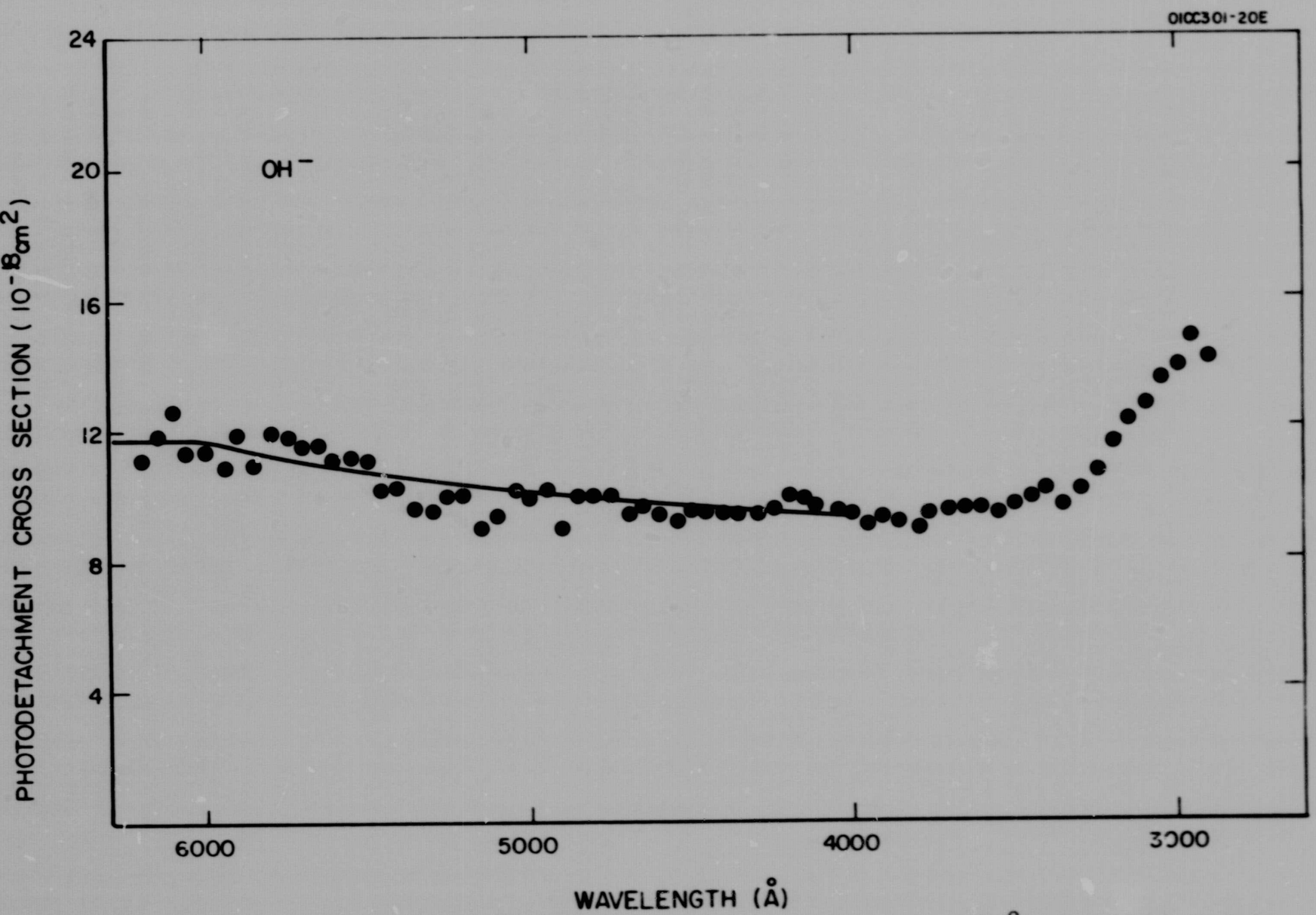

Figure 14. Photodetachment cross sections for OH^- spectral resolution 180Å half width. Solid curve refers to interpolated data by Branscomb (Ref. 26).

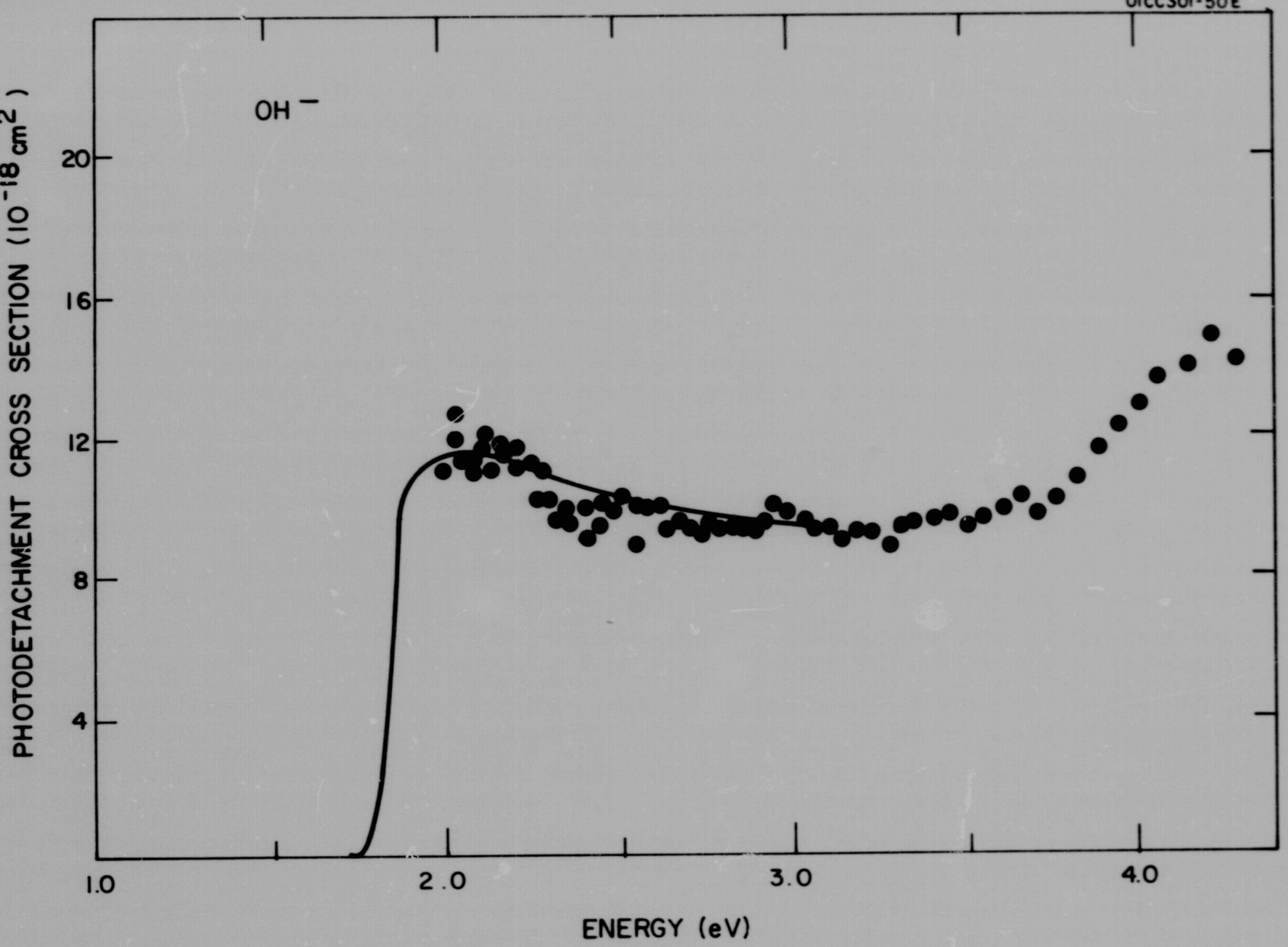

Figure 15. Photodetachment cross section for OH^-. Similar to Figure 14 but plotted versus energy.

wavelengths the photodetachment cross section rises again. Since the first excited electronic state of neutral OH lies above 4 eV above the ground state, the rise of the cross section cannot be associated with a transition to an excited state of OH. At the present time there is no knowledge about the location of excited states of OH^- which could give rise to autoionization, so that the origin of the increase of cross section values below 3400Å cannot be assessed.

F. Carbonate and Nitrate Ions

The investigation of negative ion reactions has shown that CO_3^- and NO_3^- are final products in a chain of reactions starting with O_2^- and involving upper atmospher constitutents (Ref. 1). For these reasons the photodetachment of electrons from the ions CO_3^- and NO_3^- has particular significance. The fact that these ions are final products in a series of charge transfer and ion atom interchange reactions indicates their considerable stability, and energies of about 4 eV are probably required to produce the photodetachment of electrons.

In the present work, it was attempted to observe photodetachment for CO_3^- and NO_3^-, but these attempts were unsuccessful because the ions could not be generated with sufficient intensity to obtain meaningful results for the photodetachment cross section or its upper limit. CO_3^- was generated by discharging a suitable mixture of oxygen and carbon dioxide. The maximum ion current obtained was 1×10^{-8} amps, but it soon decreased to 6×10^{-9} amps and could not be brought up again. No advantage was gained in discharging a mixture of oxygen and carbon-monoxide. NO_3^- was obtained from a discharge of air and oxygen mixture, and from a mixture of NO_2 in oxygen. In both cases, the maximum NO_3^- ion current generated was only 6×10^{-9} amps. Experiments were performed operating with the monochromator set to transmit at 3000Å (using a pyrex filter to reduce the photoelectron contribution) and with undispersed light. In no case was an unequivocal photodetachment signal observed.

IV. CONCLUSIONS

In the present work, measurements of photodetachment cross sections available previously for O^-, H^-, O_2^-, and OH^- have been extended toward shorter wavelengths. Photodetachment cross sections for NO_2^- have been obtained for the first time. Photodetachment observations for CO_3^- and NO_3^- have been attempted but have not been successful. Fehsenfeld et al. (Ref. 1) have discussed the negative ion chemistry of the D-region and have concluded that based on the available knowledge, the important steady state ions are O_2^-, CO_3^-, and NO_2^-. The steady state concentrations of O^- and O_3^- are probably too small to be significant, but NO_3^- which is formed by reactions of O_3^- with NO may become important if its lifetime is sufficiently long. The negative ions of oxygen are formed by the electron attachment reactions

$$O_2 + e + M \rightarrow O_2^- + M$$

$$O_3 + e \rightarrow O^- + O_2$$

The other ions are due to the charge transfer of O_2^- and O^- to ozone, resulting in O_3^-, which then interacts rapidly with CO_2 and NO to form CO_3^- and NO_3^-. The reaction of CO_3^- with NO gives NO_2^-. It is of interest to note that photodetachment does not appear to provide the major loss of O_2^- and O^-. As Fehsenfeld et al. have pointed out, at altitudes above 50 km, O_2^- and O^- are lost mainly by associative detachment

$$O^- + O \rightarrow O_2 + e$$

$$O_2^- + O \rightarrow O_3 + e$$

The corresponding loss rates are much higher than the photodetachment rates for O^- and O_2^- derived by Branscomb (Ref. 15) for wavelengths above 4000Å. Since the solar flux wavelength distribution favors the wavelength region above 4000Å, this statement probably remains justified even though the photodetachment cross sections for O^- and O_2^- increase by at least a factor of two at shorter wavelengths.

Photodetachment cross sections for the important ion NO_2^- are now available and have been published (Ref. 17). In the wavelength region above 4000Å, these data probably reflect a higher vibrational excitation of the NO_2^- ion. This factor should be borne in mind when applications are made to the D-region of the upper atmosphere. The cross sections are relatively low; nevertheless photodetachment of NO_2^- can represent an important process in the D-region chemistry in view of the fact that this ion

does not react with other abundant species, such as atomic oxygen, atomic nitrogen or ozone. The equally important ion CO_3^- has still eluded experimental measurement. Future experiments should therfore concentrate on this important ion and also NO_3^-. The inability in the present work to generate sufficient intensities of these ions is mainly due to a less than optimum choice of gas mixture in the ion source. Since both CO_3^- and NO_3^- are formed by reaction of O_3^-, which in turn is produced by charge transfer from O^- and O_2^- to ozone, it appears appropriate to use gas mixtures of ozone with CO_2 or NO. Working with ozone requires relatively minor additions and modifications to the existing ion source apparatus. However, it will also be necessary to reduce the noise level due to photoelectrons in the photodetachment chamber. In this respect, there exists room for improvement by a better baffling of the scattered radiation, increasing the monochromaticity of the light beam, etc.

A point of interest that cannot be revealed by photodetachment experiments directed at detecting the detached electrons, concerns the possible significance of photodissociation in the D-region of the upper atmosphere. One such process

$$O_2^- + h\nu \rightarrow O + O^-$$

has already been discussed. The energy range accessible with the present apparatus is favorable for the observation of this process as it requires about 4.1 eV. Another such process of interest is

$$CO_3^- + h\nu \rightarrow CO_2 + O^-$$

Its energy requirement can be estimated to be $\approx$ 4.1 eV from the observation of the reaction (Ref. 1)

$$O^- + CO_3 \rightarrow O_2^- + CO_2$$

which indicates that it is exothermic. The equivalent process for the NO_2^- ion

$$NO_2^- + h\nu \rightarrow NO + O^-$$

however, will require 5.6 eV on the basis of the NO_2 affinity determined here, so that it cannot be observed with the radiation energies presently available. Such processes could, in principle, explain the enhancement

in the electron density observed at morning twilight (Refs. 2, 3) since the O^- ion generated via photodissociation would quickly undergo associative detachment leading to the liberation of electrons. Laboratory experiments can decide whether the relevant cross sections for photodissociation are sufficiently large. Such experiments can be performed with the existing apparatus. For the detection of the O^- fragment, the addition of a small mass filter in the rear of the photodetachment chamber would be required, but this is a relatively minor modification since only a low mass resolution is needed and experimental specifications are not critical. An appropriate mass filter would be available for this purpose. At the present time, a prediction of cross section values of 10^{-18} to 10^{-17} cm^2 for the photodissociation processes discussed above appears reasonable.

Finally, it should be noted that recent flowing afterglow experiments (Ref. 28) have indicated that the association of O_2^- with O_2 to form O_4^- may be an important O_2^- loss process in the D-region. This event leads to subsequent reactions of O_4^- with CO_2, NO and O, and to the formation of CO_4^-, NO_3^- and O_3^-. In addition to NO_3^-, therefore, CO_4^- will require experimental photodetachment studies.

REFERENCES

1. Fehsenfeld, I.C., Schmeltekopf, A. L., Schiff, H. I., and Ferguson, E. E., Planet. Sci. 15, 373 (1967)

2. Eriksen, K. W., Holt, O., and Landmark, B., J. Atm. Terr. Phys. 18, 78 (1960); Reid, G. C., and Leinback, H., J. Atm. Terr. Phys. 23, 216 (1962); Reid, G. C., J. Geophys. Res. 66, 4071 (1961).

3. Bowhill, S. A., and Smith, L. G., COSPAR Meeting, Buenos Aires (1965).

4. Warneck, P., Final Report under Contract No. NAS5-11040, (January 1969).

5. Fite, W. L., Phys. Rev. 89, 411 (1953).

6. Whitlock, W. S. and J. F. Bounden, Proc. Phys. Soc. 75, 845 (1961).

7. Michaelson, H. B., J. Appl. Phys. 21, 536 (1950).

8. Branscomb, L. M., S. J. Smith and G. Tisone, J. Chem. Phys. 43, 2906 (1965).

9. Branscomb, L. M., D. S. Burch, S. J. Smith and S. Geltman, Phys. Rev. 111, 504 (1958).

10. Branscomb, L. M., In Atomic and Molecular Prccesses, ed. D. R. Bates, Academic Press, N. Y., p. 100 (1962).

11. John, T. L., Astrophys. J. 131, 743 (1960); Monthly Nat. Roy. Astron. Loc. 121, 41 (1960).

12. Geltman, S. and M. Krauss, Bull. Am. Phys. Soc. 5, 339 (1960).

13. Smith, S. J. and D. S. Burch, Phys. Rev. Letters 2, 165 (1959); Phys. Rev. 116, 1125 (1959).

14. Branscomb, L. M. and S. J. Smith, Phys. Rev. 98, 1028 (1955).

15. Branscomb, L. M., Am. Geophys. 20, 88 (1964).

16. Watanabe, K., J. Chem. Phys. 22, 1564 (1954).

17. Warneck, P., Chem. Phys. Letters 3, 532 (1969).

18. Pritchard, H. O., Chem. Rev. 52, 529 (1953).

19. Farragher, A. L., F. M. Page and R. C. Wheeler, Discussions Faradat Soc. 37, 203 (1964).

20. Curran, R. K., Phys. Rev. 125, 910 (1962).

21. Paulson, J., private communication.

22. Burch, D. S., S. J. Smith, L. M. Branscomb, Phys. Rev. 112, 171 (1958); 114, 1652 (1959).

23. Pack, J. L. and A. V. Phelps, J. Chem. Phys. 44, 1870 (1966).

24. Gilmore, F. R., J. Quant. Spectrosc. Radiat. Transfer. 5, 369 (1965).

25. Browne, J. C., unpublished.

26. Branscomb, L. M., Phys. Rev. 148, 11 (1966).

27. Branscomb, L. M., and S. J. Smith, unpublished.

28. Fehsenfeld, F. C., Symposium on the Physics and Chemistry of the Upper Atmosphere, Stanford Research Institute, Menlo Park, Calif. (June 1969).